

Miscibility of polyolefin blends from a Born-Green-Yvon lattice model in conjunction with small scale simulations

J. Luettmer-Strathmann* and J. E. G. Lipson

Department of Chemistry, Dartmouth College, Hanover, New Hampshire 03755

(Received 1 June 1998; revised manuscript received 28 August 1998)

The large variation in miscibility of blends of polyolefins is related to the architecture of the chain molecules. In this paper we present first results of an approach in which small scale simulations of local interactions are combined with an analytical model for the thermodynamics, the Born-Green-Yvon lattice model, to predict phase diagrams of polyolefin blends from the pure component properties. [S1063-651X(99)05102-8]

PACS number(s): 61.25.Hq, 64.75.+g, 61.43.Bn

I. INTRODUCTION

Phase separation is an important aspect of the materials science of polymer blends (see, for example, Ref. [1]), but difficult to predict from the properties of the pure components. Theoretical models for polymer blends require a value for the interaction strength ϵ_{12} between unlike segments. Recent works in the literature [2–10] make use of a comparison with experimental properties of the blend [2,4,7], Berthelot's geometric-mean combining rule [8,9], and group contribution methods [10] to estimate values for ϵ_{12} . Several authors, including Dudowicz and Freed [3] and Graessley and co-workers (cf. Ref. [6,7]), have noted the sensitivity of the phase coexistence behavior to very small changes in ϵ_{12} . By combining the recently developed [11–13] Born-Green-Yvon (BGY) lattice model for the thermodynamics of chain-molecule fluids with Berthelot's rule for ϵ_{12} , we were able to predict [14,15] thermodynamic properties of mixtures of unbranched chain-molecule fluids (*n*-alkanes and polyethylene). In this work, we modify the approach to describe systems whose components differ in local architecture.

The recent experimental work on polyolefin blends by Graessley and co-workers (cf. Ref. [6] and references therein) reveals that the short side chains of the polyolefins have a dramatic effect on their miscibility, leading to qualitatively different phase diagrams for different blends. The BGY lattice model in conjunction with the geometric mean approximation for ϵ_{12} is not able to capture these effects of local chain structure on miscibility, but only small adjustments of ϵ_{12} are required for quantitative agreement with experimental phase transition data. It therefore seems reasonable to expect that hydrocarbon blend properties can be predicted without fitting experimental data on the blends. To this end we have developed a method by which corrections to Berthelot's geometric-mean combining rule can be obtained from small scale simulations of local interactions. The procedure is illustrated here for two polyolefin blends for which experimental phase transition data are available: a blend of polyethylene (PE) with an alternating polyethylene/polypropylene copolymer (PEP) which exhibits an upper

critical solution temperature (UCST) [16], and a blend of PEP with polyisobutylene (PIB) which exhibits a lower critical solution temperature (LCST) [17]. The architecture of the polymers is schematically represented in Fig. 1. While the interaction potentials are known to vary with the number of covalently bonded carbon atoms (cf. Ref. [4]), we focus here on the role of geometry and leave the question of different interaction strengths for sites on the same molecule to future work.

The remainder of the paper is organized as follows: After a brief outline in Sec. II, of the BGY lattice model and its application to the two polymer blends considered here, we describe a method to determine geometric corrections to Berthelot's rule in Sec. III. In Sec. IV we compare predicted phase diagrams with experimental data and show that the BGY lattice model in conjunction with the corrected mixed interaction yields qualitatively correct results for phase separation in the polyolefin blends.

II. APPLICATION OF THE BGY LATTICE MODEL TO COMPRESSIBLE POLYMER BLENDS

In the BGY lattice model, a molecule of species *i* is assumed to occupy r_i contiguous sites on a lattice having coordination number z and a volume $V = vN_0$, where N_0 is the number of lattice sites and v is the volume per site. As in earlier work [11,12,14], we set $z=6$ corresponding to the simple cubic lattice. The site fractions ϕ_i , ϕ_h , and ϕ are defined as $\phi_i = r_i N_i / N_0$, $\phi_h = N_h / N_0$, and $\phi = 1 - \phi_h$, where N_i is the number of molecules of component *i* and N_h is the number of empty sites or holes. Each molecule of species *i* has $q_i z = r_i(z-2) + 2$ interaction sites, leading to the definition of concentration variables $\xi_i = q_i N_i / (N_h + \sum_j q_j N_j)$ and $\xi_h = N_h / (N_h + \sum_j q_j N_j)$ which account for the nearest-neighbor connectivity of the molecules. The interaction energy associated with nonbonded nearest neighbors of the same species is ϵ_{ii} , while ϵ_{ij} corresponds to interactions

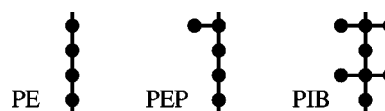


FIG. 1. United atom representation of the polyolefins considered in this work; shown are the repeat units with four carbon atoms in the backbone.

*Present address: Department of Physics, University of Akron, Akron, OH 44325-4001.

TABLE I. System-dependent parameters for the polyolefins considered in this work.

Components	PEP	PE	PEP	PIB
M_w	29450	23560	59900	38600
v (L/mol)	0.00924	0.00924	0.00957	0.00957
r_i	3467.30	2770.83	6809.14	4143.47
ϵ_{ii} (J/mol)	-2000.0	-1977.5	-2000.0	-2208.1
ϵ_{geo} (J/mol)	-1988.718		-2101.476	
$g_0 - 1$	-3.51×10^{-4}		9.09×10^{-4}	

between unlike nearest neighbor segments. Using the Born-Green-Yvon integral equation approach, Lipson [13] derived expressions for the probabilities of the different types of contacts, and from there an expression for the Helmholtz free energy of compressible fluids.

When applied to the pure polyolefins, the BGY lattice model has three system-dependent parameters, r_i, v_i , and ϵ_{ii} , which are *effective* characteristic parameters of the fluid. We determined these parameters, from a comparison with experimental pressure volume temperature (PVT) [6,18] data in a common pressure ($10 \text{ MPa} \leq P \leq 100 \text{ MPa}$) and temperature ($400 \text{ K} \leq T \leq 500 \text{ K}$) range. Except for the highest pressure at low temperatures, the BGY lattice model describes the experimental data well within their experimental uncertainty [18]; the reduced χ^2 does not exceed a value of 0.7 for any of the fits. For the description of the blends, a value has to be assigned to the volume per lattice site. In this work we employ the average $v = (v_1 + v_2)/2$, and rescale the segment numbers r_i so as to keep the hard core volume $r_i v_i$ constant: $r_i \rightarrow r_i v_i / v$. While the molecular mass M_w of a polymer has little effect on the PVT surface of a pure melt (we set $M_w = 170\,000$ in the fits), it does affect the phase diagrams of the blends. Since the segment number r_i is proportional to the molecular mass [14], the relationship $r_i(M'_w) = r_i(M_w) M'_w / M_w$ is used to obtain a value of r_i appropriate for a polymer of molecular mass M'_w . Finally, Berthelot's geometric-mean combining rule is given by

$$\epsilon_{\text{geo}} = -\sqrt{\epsilon_{11}\epsilon_{22}}. \quad (1)$$

The parameter values for the polyolefin blends considered here are collected in Table I.

III. SMALL SCALE SIMULATIONS OF THE MIXED INTERACTIONS

To capture the effect of local architecture on the mixed interaction strength we evaluate possible interactions between sections of two polyolefin molecules in united atom representation, where we focus on configurations with straight backbones in this work (cf. Fig. 2). For each of the molecules, consider a straight section composed of three repeat units with given (not necessarily identical) side group arrangements. The repeat unit in the middle is the section of interest in each case, while the attached units represent the rest of the (long) chains.

The section of interest of the first molecule is fixed to the origin of a simple cubic lattice, and aligned with the z axis.

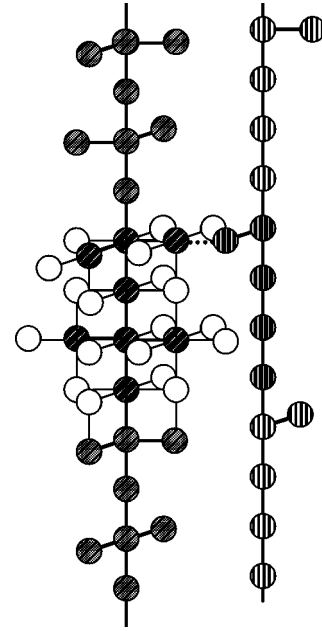


FIG. 2. Example of a combined configuration with PIB as the fixed molecule on the left and PEP as the mobile one on the right. The darker shaded spheres indicate sites belonging to the sections of interest, while the lighter colored spheres represent sites on the attached repeat units. The section of interest of the PIB segment has $s_f = 8$ sites corresponding to a maximum number of $c_m = 32$ contacts, indicated by the light lines and the dotted line. There are $n_t = 24$ nonbonded nearest neighbor sites to the section of interest of PIB, indicated by the white spheres, one of which is occupied by a site of interest of the mobile PEP segment. In this combined configuration, the mobile segment occupies one nearest neighbor site of the fixed segment of interest, i.e., $o_k = 1$, and makes one contact indicated by the dotted line, i.e., $c_k = 1$.

The total number n_t and the coordinates of the nonbonded nearest neighbor (nn) sites are determined as is the maximum number $c_m = 4s_f$ of possible contacts, where s_f denotes the number of lattice sites occupied by the fixed section of interest. The second molecule is mobile: it is rotated and translated so that its section of interest makes contact with the section of interest of the fixed molecule without overlap between the molecules. The number o_k of nn sites of the fixed section of interest occupied by the mobile chain are counted as are the number of established contacts c_k between the two chains. The last two steps are repeated until all possible combined configurations of the two chains are exhausted; then the whole procedure is repeated with different arrangements of the side groups of the molecules. For the results presented here, all side group configurations of the sections of interest and their attachments were considered (exact enumeration procedure). To avoid excessive computation times for systems with a larger number of configurations of the individual molecules, due to longer side chains or bent backbones, for example, a Monte Carlo method can be used to generate representative samples of the individual polymer configurations. The results of the simulation are statistics on the number m_k of combined configurations corresponding to a given pair (o_k, c_k) of occupied nn sites and established contacts.

To determine the energy of a combined configuration, we assume that the remaining $n_t - o_k$ nn sites are filled randomly

to a density of ξ . Here $\xi = 2\phi/(3-\phi)$ is the contact density for infinitely long chains corresponding to a total filling fraction of ϕ . [Assuming infinite chains here has negligible effect on the simulation results since the main density dependence is divided out when the interaction energy per contact is determined, cf. Eq. (4), but it has the advantage of making the simulation results independent of molar mass.] Accordingly, the energy E_k for a set of combined configurations (o_k, c_k) is given by

$$E_k = \epsilon_{\text{geo}} \left(c_k + \frac{(n_t \xi - o_k)(c_m - c_k)}{n_t - o_k} \right). \quad (2)$$

The two contributions to the energy E_k in Eq. (2) are due to contacts between the fixed and mobile segments and between the fixed segment and its randomly filled nearest neighbor sites, respectively. For a consistent evaluation of results for the different repeat units, with their different numbers n_t of nn sites, we employ the same number $n_t = 24$ for each polyolefin in Eq. (2) and rescale the maximum number of contacts according to $c_m \rightarrow 24c_m/n_t$.

The probability P_k of a given energy E_k and the average energy \bar{E} depend on the temperature T through

$$P_k = m_k e^{-\beta E_k} / \sum_k m_k e^{-\beta E_k}, \quad \bar{E} = \sum_k E_k P_k, \quad (3)$$

where m_k is the multiplicity of the combination (o_k, c_k), $\beta = 1/RT$, R is the universal gas constant, and E_k is measured in J/mol. Dividing \bar{E} by ξc_m , where ξc_m is the number of contacts for the case in which all the nonbonded nn sites of the section of interest are filled randomly to a density of ξ , yields an interaction energy per contact:

$$\bar{\epsilon}_{12} = \bar{E} / (\xi c_m). \quad (4)$$

By changing the roles of the fixed and the mobile chains and repeating the procedure, a second value $\bar{\epsilon}_{21}$ is obtained. The average $(\bar{\epsilon}_{12} + \bar{\epsilon}_{21})/2$ represents a value for the mixed interaction strength at a given temperature and filling fraction. Since it includes the effects of the local architecture, it is expressed in terms of Berthelot's value ϵ_{geo} and a geometric correction factor g :

$$(\bar{\epsilon}_{12} + \bar{\epsilon}_{21})/2 \equiv g \epsilon_{\text{geo}}. \quad (5)$$

For straight, unbranched chains all nn sites yield a single contact when occupied: setting $c_k = o_k$ for each k and $c_m = n_t$ in Eq. (2) yields $E_k = \epsilon_{\text{geo}} c_m \xi$ for all k , so that Eqs. (3)–(5) imply $g = 1$. Hence there is no geometric correction for the mixed interactions between two straight, unbranched, chain molecules. Chains with side groups, on the other hand, have “special” nn sites whose occupation establishes more than one contact per site. Mixed interactions are (dis) favored compared to the geometric-mean approximation, i.e., $g > 1$ ($g < 1$), if the molecules can(not) take advantage of each others special sites in many combined configurations. At very low temperature, the energetically favorable combined configurations always outweigh the unfavorable ones in Eq. (3), so that g increases with decreasing temperature and that $g > 1$ for $T \ll T^*$, where $T^* = \epsilon_{\text{geo}}/R$. Finally, independent of

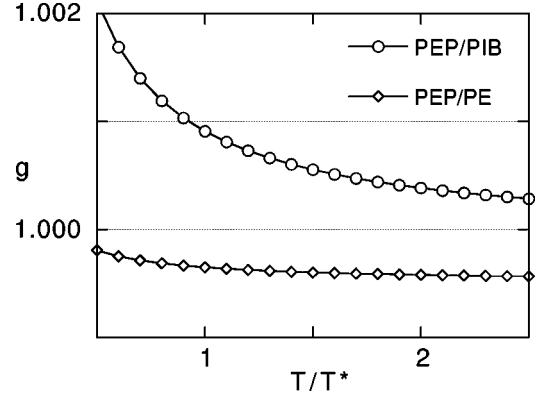


FIG. 3. The geometric correction g as a function of reduced temperature for the blends considered in this work at a filling fraction of $\phi = 0.85$.

chain architectures, $g = 1$ for $\phi = 1$, since all nn sites are occupied and all possible contacts are saturated when the lattice is completely filled.

In Fig. 3 we present the geometric correction g as a function of reduced temperature T/T^* for interactions between PEP and PE molecules and between PEP and PIB molecules at a filling fraction of $\phi = 0.85$. The geometric corrections are larger than unity for PEP/PIB and smaller than unity for PEP/PE interactions, corresponding to enhanced and reduced miscibility compared to the geometric mean prediction, respectively.

In the application of the BGY lattice model to polyolefin blends a single value for the mixed interaction strength,

$$\epsilon_{12} \equiv g_0 \epsilon_{\text{geo}}, \quad (6)$$

is employed, and requires the extraction of a single value for the geometric correction g_0 from the simulation results. For g_{sim} we choose the value of g at the characteristic temperature of the blend, i.e., $T/T^* = 1$, and a filling fraction $\phi = 0.85$, where the choice of ϕ is motivated by the typical hole concentrations encountered in the PVT data of the pure components. Values for g_0 are included in Table I.

IV. RESULTS AND DISCUSSION

To demonstrate the effect of the geometric correction g_0 we investigate phase separation in the polyolefin blends. In Table II we present a comparison of experimental results [16,17] with predictions from the BGY lattice model in con-

TABLE II. Experimental and predicted phase transition temperatures T_{tr} at atmospheric pressure for the polyolefin blends of Table I at the indicated PEP mass fractions c_{PEP} .

	Experiment	$\epsilon_{12} = \epsilon_{\text{geo}}$	$\epsilon_{12} = g_0 \epsilon_{\text{geo}}$
PEP/PE, $c_{\text{PEP}} = 0.5$			
type of phase diagram	UCST [16]	miscible	UCST
$T_{\text{tr}}(\text{K})$	421 ± 1 [16]	–	465
PEP/PIB, $c_{\text{PEP}} = 0.2$			
type of phase diagram	LCST [17]	LCST	LCST
$T_{\text{tr}}(\text{K})$	318 ± 5 [17]	130	311

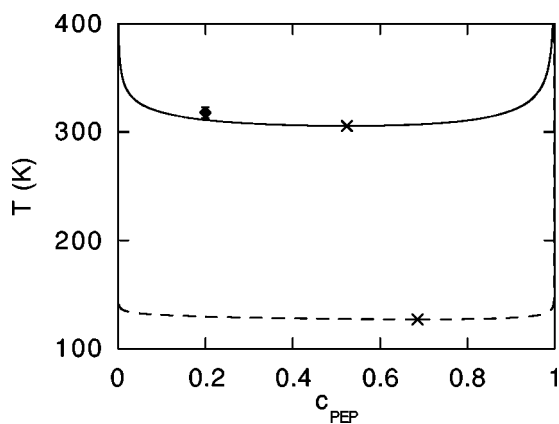


FIG. 4. Phase coexistence in the PEP/PIB blend of Table I at a pressure of 0.1 MPa. The solid diamond indicates an experimental value [6] for the phase transition temperature. The solid line is predicted with the aid of the geometric correction g_0 , $\epsilon_{12} = g_0 \epsilon_{\text{geo}}$, while the dashed line is calculated with $\epsilon_{12} = \epsilon_{\text{geo}}$. The crosses mark the LCST's and c_{PEP} is the mass fraction of PEP.

junction with the geometric-mean combining rule, $\epsilon_{12} = \epsilon_{\text{geo}}$, and the geometric corrections, $\epsilon_{12} = g_0 \epsilon_{\text{geo}}$, respectively, where the parameter values of Table I have been used. For the PEP/PE blend, cloud-point measurements by Bates, Schulz, and Rosedale [16] indicate an UCST at 421 ± 1 K. While the geometric mean approximation yields a prediction of complete miscibility, the application of the geometric correction g_0 changes the prediction qualitatively and yields a UCST at 465 K. Cloud-point determinations of partially deuterated samples by Krishnamoorti *et al.* [17] indicate a LCST phase diagram for the PEP/PIB system. In this case, the prediction based on the geometric-mean combining rule is qualitatively correct, but the application of the geometric correction g_0 leads to a quantitative improvement. In Fig. 4 we present the predicted coexistence curves for PEP/PIB blends.

It is interesting [19–21] to investigate the effect of pressure on the miscibility of polymer blends. In Fig. 5 we present predictions from the BGY lattice model with geometric correction for the pressure variation of the upper and lower critical solution temperatures of PEP/PE and PEP/PIB blends. In qualitative agreement with experimental results for other polyolefin blends [20,21], we find that increasing the pressure reduces the miscibility of the blend exhibiting a UCST, and increases the miscibility of the LCST blend.

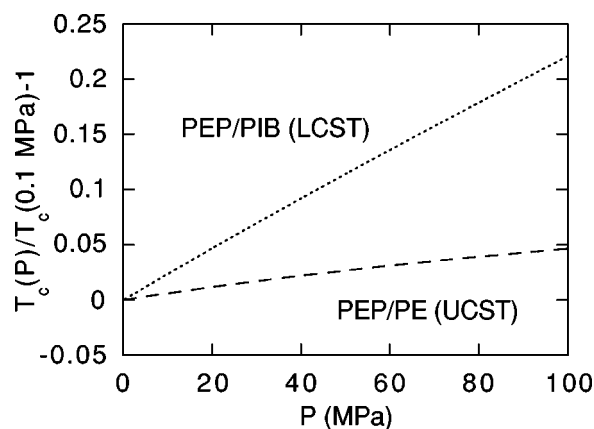


FIG. 5. Relative pressure variation of the critical temperatures of the PEP/PE and PEP/PIB blends of Table I as predicted with the aid of the geometric correction g_0 .

Considering the effect of the molecular mass of the components we find, in agreement with experimental observation [17], that the miscibility for both types of blends decreases with increasing molecular mass, but that this effect is much more pronounced in UCST blends.

In summary, the BGY lattice model in conjunction with the simulation results for the geometric correction [Eq. (6)], yields qualitatively correct predictions for phase separation in polyolefin blends with either UCST or LCST phase diagrams. The results presented here are obtained with the aid of a simulation method which allows the prediction of these hydrocarbon blend properties from information about the pure components alone. The agreement between theory and experiment is not yet quantitative, however. Currently, we are studying a larger set of blends with polyolefins of different architectures to gain experience and improve on the determination of the geometric correction g_0 . In future work, it will be interesting to include the effect of flexibility of the chains and to consider different interaction potentials for sites on the same molecule.

ACKNOWLEDGMENTS

The authors would like to thank D. J. Lohse for supplying PVT data for the polymers, and M. P. Taylor for many useful discussions. This research was supported by grants from the National Science Foundation (Grant No. DMR-9730976) and the Camille and Henry Dreyfus Foundation.

[1] *Polymer Blends*, edited by L. A. L. Kleintjens, special issue of *Macromol. Symp.* **112** (1996).
 [2] J. Dudowicz and K. F. Freed, *Macromolecules* **28**, 6625 (1995).
 [3] J. Dudowicz and K. F. Freed, *Macromolecules* **29**, 8960 (1996).
 [4] K. W. Foreman and K. F. Freed, *Macromolecules* **30**, 7279 (1997).
 [5] K. W. Foreman, K. F. Freed, and I. M. Ngola, *J. Chem. Phys.* **107**, 4688 (1997).

[6] R. Krishnamoorti, W. W. Graessley, G. T. Dee, D. J. Walsh, L. J. Fetters, and D. J. Lohse, *Macromolecules* **29**, 367 (1996).
 [7] J. K. Taylor, G. Debenedetti, W. W. Graessley, and S. K. Kumar, *Macromolecules* **29**, 764 (1996).
 [8] J. J. Rajasekaran, J. G. Curro, and J. D. Honeycutt, *Macromolecules* **28**, 6843 (1995).
 [9] C. Singh and K. S. Schweizer, *Macromolecules* **30**, 1490 (1997).
 [10] T. M. Ellis, *Macromol. Symp.* **112**, 47 (1996).

- [11] J. E. G. Lipson and S. S. Andrews, *J. Chem. Phys.* **96**, 1426 (1992).
- [12] J. E. G. Lipson and P. K. Brazhnik, *J. Chem. Phys.* **98**, 8178 (1993).
- [13] J. E. G. Lipson, *Macromol. Theory Simul.* **7**, 263 (1998).
- [14] J. Luettmer-Strathmann and J. E. G. Lipson, *Fluid Phase Equilib.* **150–151**, 649 (1998).
- [15] J. Luettmer-Strathmann, J. A. Schoenhard, and J. E. G. Lipson, *Macromolecules* (to be published).
- [16] F. S. Bates, M. F. Schulz, and J. H. Rosedale, *Macromolecules* **25**, 5547 (1992).
- [17] R. Krishnamoorti, W. W. Graessley, L. J. Fetters, R. T. Garner, and D. J. Lohse, *Macromolecules* **28**, 1252 (1995).
- [18] D. J. Walsh, W. W. Graessley, S. Datta, D. J. Lohse, and J. L. Fetters, *Macromolecules* **25**, 5236 (1992).
- [19] S. Janssen, D. Schwahn, K. Mortensen, and T. Springer, *Macromolecules* **26**, 5587 (1993).
- [20] B. Hammouda, N. P. Balsara, and A. A. Lefebvre, *Macromolecules* **30**, 5572 (1997).
- [21] M. Rabeony, D. J. Lohse, R. T. Garner, S. J. Han, W. W. Graessley, and K. B. Migler, *Macromolecules* **31**, 6511 (1998).